

CORRELATION OF LOCAL HEAT FLUX FROM
INCLINED VOLUME-HEATED POOLS IN BUBBLY FLOW

By

G. A. Greene
N. Abuaf
O. C. Jones, Jr.

Department of Nuclear Energy
Brookhaven National Laboratory
Upton, New York 11973

Paper Presented at
19th National Heat Transfer Conference
Orlando, Florida

July 27-30, 1980

THIS DOCUMENT CONTAINS
POOR QUALITY PAGES

* Work performed under the auspices of the United States Nuclear Regulatory
Commission.

8006200

014

ABSTRACT

Local and average heat transfer from volume-boiling pools in the two-phase bubbly flow regime to vertical and inclined flat boundaries were measured. The experimental technique and newly developed gold electroplated microthermocouples to make the measurements are described. A modification to the Boussinesq approximation for liquids is outlined which includes the effect of the average void fraction in a modified Rayleigh number. Heat transfer to vertical and inclined surfaces is correlated in a fashion similar to natural convection in the bubbly flow regime. The empirical correlations derived and their ranges of applicability are

$$Nu(x) = \begin{cases} (1.41 \pm .23) Ra^{0.25} & Ra^* \leq 7 \times 10^{11} \\ (.0234 \pm .002) Ra^{0.40} & Ra^* > 7 \times 10^{11} \end{cases}$$

and

$$\overline{Nu} = \begin{cases} (1.54 \pm .08) Ra^{0.25} & Ra^* < 1.9 \times 10^{11} \\ (.0314 \pm .0016) Ra^{0.40} & Ra^* > 1.9 \times 10^{11} \end{cases}$$

where the error ranges indicated represent the root mean square deviation in determination of the correlation coefficient. It was found that these new correlations agreed in general with those based on average heat transfer data obtained by Gabor et al [2]. The data from Ref. 3, however, were found to lie significantly below the present data on an average as well as local basis.

NONENCLATURE

a	Test wall thickness
BN	Boron nitride
g	Gravitational acceleration
Gr*	Modified Grashof number (defined in Eq. 1)
h	Heat transfer coefficient
h _{fg}	Heat of vaporization

H	Boiling depth
H ₀	Static depth
j _{g∞} /U _∞	Dimensionless superficial vapor velocity, $\dot{q}''' H_0 / \rho_v h_{fg} U_\infty$
k	Thermal conductivity
L	Length of heat transfer surface
Nu	Nusselt number, hx/k
Pr	Prandtl number
\dot{q}'''	Volumetric power density
Ra*	Modified Rayleigh number, Gr* Pr
T	Temperature
U _∞	Bubble terminal rise velocity 1.53 (gσ(ρ _l - ρ _v)/ρ _l ²) ^{1/4}
x	Coordinate along boundary layer

Greek Symbols

$\bar{\alpha}$	Average void fraction, 1 - H ₀ /H
η	Variable of integration (Eq. 6)
θ	Angle of inclination from vertical
ν	Kinematic viscosity
ρ	Density
σ	Surface tension

Subscripts

av	Average
B	Back
eff	Effective
F	Front

l	Liquid
sat	Saturation
v	Vapor
*	Bulk fluid

INTRODUCTION

Accurate modeling of the heat transfer distribution to vertical and inclined boundaries from liquid pools boiling due to internal heat generation is of particular importance in analysis of core disruptive accidents in nuclear power reactors as well as in certain chemical reactor applications. The boiling hydrodynamics are sensitive to the convective heat losses and, in turn, the heat transfer magnitude and distribution has been shown previously to be dependant upon the boiling flow regime.

It has been previously shown⁽⁵⁾ that the local heat loads may vary along the boundary by as much as a factor of five or more. As a result, there is a need for accurate heat transfer models to predict average and local heat loads from volume-boiling pools to bounding vertical surfaces.

It is the purpose of this paper to present new data and correlations for both local and average heat transfer coefficients representing a substantial improvement over those previously available.

PREVIOUS INVESTIGATIONS

There have been three prior attempts to measure heat transfer from volumetrically boiling pools to vertical boundaries.

In the earliest attempt, Stein et al⁽¹⁾ measured average boundary heat transfer from a volume-boiling pool of NaCl. A thermocouple was buried in a dead-end hole for surface temperature measurement and average boundary heat flux was inferred. It was postulated that the boundary heat flux was bounded by asymptotes of free and forced convection similar to single phase flow. Between the asymptotes, mixed convection was assumed to exist. The only correlations proposed were conventional heat transfer correlations for single phase flow for the asymptotic cases.

The same type of experiment was repeated by Gabor et al⁽²⁾ in which average heat transfer from a boiling ZnSO₄ solution to vertical boundaries was measured; this time the surfaces (electrodes) were split to measure average heat transfer to upper and lower segments. The heat flux was inferred from the enthalpy rise of the coolant in the brazed copper cooling coils on the electrodes. The upper to lower heat flux ratio was found to be approximately 2:1 for natural convection pools and approximate unity for turbulent agitated pools. These regimes have since been identified as the bubbly and churn turbulent flow regimes. The average heat transfer data were correlated as forced convection with a Reynolds number based upon the vapor superficial velocity and the pool depth.

Gustavson et al⁽³⁾ subsequently investigated the distribution of boundary heat transfer from volume-boiling pools to a test wall which was segmented into a number of thermally isolated segments. Each segment was instrumented for calorimetry to determine the local heat flux distribution along the wall. The test plate was suspended into the pool from above and electrically (and thermally) insulated from the electric field with a teflon sheet covering. It was observed that the distribution of heat transfer resembled boundary layer convection. They proposed that the free and forced convection correlations previously used by Stein be asymptotically matched to describe mixed convection in the region in between.

The Gustavson data⁽³⁾ represented the first local heat transfer data from volume-boiling pools. The present authors conceived that boundary heat transfer could be simply modeled on the basis of natural convection, where the Boussinesq approximation, which represents the density difference across the boundary layer in terms of a temperature difference was modified to include the effect of the average void fraction to represent the true density difference across the boundary layer. This approximation is outlined in Appendix A and takes the approximate form

$$Gr^* \sim \frac{g_{eff} \alpha x^3}{\nu^2} \quad (1)$$

where the effective gravitational acceleration, $g_{eff} = g \cos \theta$, is used to account for wall inclination effects. In the results presented herein, the average pool void fractions, $\bar{\alpha}$, were used since local values were not available.

Local and average heat transfer correlations were determined for the data of Gustavson⁽³⁾ based on this approximation. These were given by (4)

$$Nu(x) = (0.78 \pm 0.35)(Gr^*Pr)^{0.25} \quad (2)$$

and

$$Nu = (1.07 \pm 0.30)(Gr^*Pr)^{0.25} \quad (3)$$

Less than 3% difference was found in (2) when the local void fraction was used as opposed to the pool averaged value. However, the standard deviation decreased by over 30% due to the improved accuracy in Gustavson's measurement of average vs local void fractions, the stated RMS error in the latter being + 10%. The correlation for the average heat transfer was found to be substantially lower than that obtained for Gabor's data⁽²⁾ where the correlation coefficient was 1.59 ± 0.33 , even though the scatter was similar. It should be noted that the RMS scatter in (2) and (3) is of the same order quoted by Gustavson⁽³⁾ of 40% relative. This scatter, however, is too great to permit any firm conclusions concerning the mechanistic nature of the heat transfer processes. No information was available concerning inclined boundaries. In order to resolve these uncertainties, the experiment to be described was undertaken.

EXPERIMENT

A rectangular pool, shown schematically in Fig. 1, was constructed of lexan; copper electrodes were machined and recessed into the walls. The test wall consisted of a lexan frame and a boron nitride test sheet (nominal size: length 30.48 cm, width 12.70 cm, thickness 1.27 cm); the BN sheet was rabbeted and pressed into position flush with the lexan to eliminate nucleation sites. The test wall was sandwiched between the electrode walls and rounded at the base. In this way, the test surface was an integral part of the boundary which could be inclined at any angle from vertical (90°) to at least 60° . Boron nitride was used for the test surface since it is an electrical insulator as well as a good thermal conductor. This eliminated the need for insulating the wall from the pool and avoided the difficulty of temperature extrapolation experienced in Ref. 3. A separate coolant water loop was constructed for heat transfer at the rear of the BN test wall to transfer the convective heat flux from the pool. It was designed so as not to affect the temperature pattern in the wall, to minimize the coolant temperature rise, and to eliminate problems associated with discreet cooling coils. A vertical traversing impedance probe was used to measure static and boiling pool height for calculation of average void fraction.

A special thermocouple concept was developed specifically to improve upon the temporal and spatial uncertainty in the temperature measurements which was responsible for the majority of the experimental error in the previous investigations. The BN was instrumented with chromel-alumel thermocouples for local heat transfer measurements. The thermocouples were 0.025 cm diameter stainless steel-clad microthermocouples, machined flat at the junction and gold plated with ~ 0.003 cm of gold forming the hot junction across the isolated chromel and alumel leads. A schematic of the cross-sectionally polished and gold plated microthermocouples is shown in Fig. 2. The thermocouples were individually calibrated at the ice point and steam point taking local barometric pressure into account and the average calibration data for each was compared to NBS type K data. It was found that all the gold plated thermocouples calibrated to within $\pm .07$ C from the steam to the ice point. The microthermocouples were then cemented into 26 locations in the BN wall, 19 on the front at 1.27 cm intervals, and 7 on the back at 3.81 cm intervals with copper oxide cement. They were installed in such a manner that the measuring junction was flush with the wall surface within an estimated $\pm .003$ cm tolerance and cemented in place under a microscope. The gold plated junction thus comprised part of the test wall surface. Heat losses along the thermocouple sheath were negligible since the leads were immersed in the plate at least 50 diameters, and the thermal conductivities of the stainless steel and boron nitride were similar.

By far the biggest difficulty occurred early in the experiment due to electrochemical attack on the thermocouples. This was caused by improper thermocouple connection to the measurement system causing slight electrical current to flow. Until this was rectified, the problem necessitated replacements and recalibrations. Slight additional errors in

excess of the estimated $\pm 3\%$ in heat transfer coefficient (Appendix B) were incurred due to problems associated with cleanly removing and re-cementing the new thermocouples.

Additional difficulties were encountered due to slight swelling of the boron nitride plate and resultant stress induced by the confinement of the holder. Ridges would form and then flaking would occur. This event was not expected or explained by the material vendor but was eliminated by replacing and stress relieving the plate in its holder.

Experiments were performed for boiling pools in the bubbly flow regime. This regime covered the range of dimensionless superficial vapor velocity, $j_{g\infty}/U_{\infty}$, up to unity, at which point a flow regime transition occurred from bubbly to churn turbulent flow.

In all cases, to achieve maximum spatial resolution, the amount of liquid in the pool (collapsed liquid depth) was maintained just sufficiently to keep the top of the boiling liquid-vapor mixture just at the top of the boron nitride plate. Several additional runs were, however, undertaken with lesser amounts of liquid and lower overall depth. No significant differences in the data were observed. In addition, the effects of altering the heat removal coolant flow rate and location of the vertical return fluid distribution plate with respect to the heat transfer surface were found to be negligible for those conditions utilized. It was found, however, that if the distribution plate was moved too close to the heat transfer surface ($< \sim 12-15$ cm) effects were felt. For each run, the average void fraction was measured for use in calculating the average two-phase film density difference in the Rayleigh number. Measured viscosity and density properties of the $ZnSO_4$ solution were used in evaluating the film properties for the heat transfer correlations.

RESULTS

Local Heat Transfer. Local heat transfer coefficients from the volumetrically boiling pool to the instrumented test surface were measured at nineteen locations along the vertical axis. The transient temperature response of each thermocouple was sampled at a rate of twenty hertz until the running standard deviation of the fluctuating temperature converged or the number of samples exceeded a preset limit. The heat transfer coefficient was calculated as indicated below:

$$h(x) = \frac{k_{BN}(T_F(x) - T_B(x))}{a \cdot (T_{sat} - T_F(x))} \quad (4)$$

The front wall temperature measurements were used directly. The equivalent back wall local temperature was obtained by linear interpolation between the seven back wall measurements. A typical distribution of temperature at a fixed location on the test plate is shown in Figure 3. The temperature distribution is Gaussian about the mean temperature (~ 92 C) with a standard deviation nominally approximately 2 C. The observation that the temperature is always less than the saturation temperature (~ 102 C for the $ZnSO_4$ solution) was

taken as confirmation that boundary heat transfer in the bubbly flow regime is through an attached wall boundary layer as previously assumed. Each experimental run was repeated at least once to examine reproducibility. It was found that the measured heat transfer coefficient at a particular location was reproducible within approximately 5% under nearly identical conditions.

The statistical analysis of the local heat transfer data resulted in the correlations below:

$$Nu(x) = (1.41 \pm .23) Ra^*(x)^{0.25}, Ra^* \leq 7 \times 10^{11} \quad (5a)$$

and

$$Nu(x) = (.0234 \pm .0020) Ra^*(x)^{0.40}, Ra^* > 7 \times 10^{11} \quad (5b)$$

In this case the local Rayleigh number is based on the average pool void fraction since local values were not available. Little difference was found between using local and average values of α in correlating Gustavson's data⁽³⁾.

Average Heat Transfer. The average heat transfer coefficient was evaluated by integrating the local distribution as

$$h_{av} = \frac{1}{L} \int_0^L h(n) dn \quad (6)$$

and the statistical analysis of the average heat transfer data resulted in the correlations below and plotted in Figure 4:

$$Nu = (1.54 \pm .08) Ra^*(L)^{0.25}, Ra^* \leq 1.9 \times 10^{11} \quad (7a)$$

$$Nu = (.0314 \pm .0016) Ra^*(L)^{0.40}, Ra^* > 1.9 \times 10^{11} \quad (7b)$$

The range of applicability of these correlations and the cumulative uncertainty assigned from detailed error analysis⁽⁴⁾ are listed in Table 1. The standard deviation shown is the deviation calculated in the correlation coefficient. The points indicated as "Transition" represent experiments performed which began to undergo hydrodynamic transition from bubbly to churn turbulent flow. All properties used in the empirical correlations are liquid properties at the film temperature.

$$T_{film} = \frac{T_{sat} + T_{F,av}}{2} \quad (8)$$

DISCUSSION

The behavior of the local wall temperature distribution as well as the nature of the modified convection correlation is taken as confirmation of the existence of a stable wall boundary layer in the bubbly flow regime. Although not shown, it has been observed that in some cases, under churn turbulent flow conditions, the local wall transient temperature response function behaves significantly differently. Instead of the nearly Gaussian distribution shown in Figure 3 with small standard deviation (~ 2 C) and zero skewness, the standard deviation in churn turbulent flow is large ($\sim 10 - 20$ C) and the distribution is skewed up to the saturation temperature. These observations indicate that the boundary layer in churn turbulent flow may be undergoing periodic destruction and renewal as manifested in intermittent saturation conditions at the wall, and will be the subject of a following report.

The correlation of average boundary heat transfer compares favorably with the correlation of the data from Ref. 2, but a large discrepancy exists with respect to the data of Ref. 3. Application of the $2 \frac{1}{2} \sigma$ band to the data of Ref. 3 more than encompasses the present data although the reverse is not true. There is, however, no explanation at the present time why the Gustavson heat transfer data⁽³⁾ are so much lower on the average than those of Gabor⁽²⁾ and those presented herein.

Both the local and average heat transfer data were successfully correlated on the basis of modified natural convection previously described. For the local data correlation, the uncertainty was approximately 10-15%; for the average data correlation, the uncertainty was approximately 5%. This represents a significant improvement over previously available models as well as confirmation of the applicability of the effective gravitational component, $g \cos \theta$, for the case of inclined vertical boundaries.

The gold plated microthermocouples that were developed demonstrated high spatial and temperature resolution. Reliability and accuracy have been demonstrated through long term use in contact with a high voltage, high current AC field. Temperature calibration was uniform within $\pm .07$ C and temporal response has been observed to be high, although no quantitative information exists for frequency response at this time. It is expected that these thermocouples will find a wide variety of applications in the future and permit refinement of existing data as shown in this investigation.

The gold plated microthermocouples that were developed demonstrated high spatial and temperature resolution. Reliability and accuracy have been demonstrated through long term use in contact with a high voltage, high current AC field. Temperature calibration was uniform within $\pm .07$ C and temporal response has been observed to be high, although no quantitative information exists for frequency response at this time. It is expected that these thermocouples will find a wide variety of applications in the future and permit refinement of existing data as shown in this investigation.

ACKNOWLEDGEMENTS

The authors would like to thank Ms. Marisa Canner for typing the manuscript. This work was performed under the auspices of the United States Nuclear Regulatory Commission.

REFERENCES

1. Stein, R. P., Hesson, J. C., and Gunther, W. H., "Studies of Heat Removal From Heat Generating Boiling Pools," ANS Fast Reactor Safety Conference, CONF-740401, pp 865-880 (April 1974).
2. Gabor, J. D., Baker, L., Jr., Cassulo, J. C., and Mansoori, G. A., "Heat Transfer from Heat Generating Boiling Pools," ASME-AIChE National Heat Transfer Conference, St. Louis, MO., pp 78-80 (1976).
3. Gustavson, W. R., Chen, J. C., and Kazimi, M. S., "Heat Transfer and Fluid Dynamic Characteristics of Internally Heated Boiling Pools," BNL-NUREG-50722 (September 1977).

4. Greene, G. A., Abuaf, N., Jones, O. C., Jr., and Schwarz, C. E., "Heat Removal Characteristics of Volume-Heated Boiling Pools With Inclined Boundaries," BNL-NUREG-26325 (May 1979).
3. Greene, G. A., Abuaf, N., Jones, O. C., Jr., and Schwarz, C. E., "Heat Removal Characteristics of Volume-Heated Boiling Pools With Inclined Boundaries in Bubbly Flow Regime," ASME Paper No. 79-HT-99, 18th National Heat Transfer Conference (August 1979).

$$\frac{\sigma_h}{h} = \left[\left(\frac{\sigma_{k_{BN}}}{k_{BN}} \right)^2 + \frac{\sigma_{T_F}^2 + \sigma_{T_B}^2}{(T_F - T_B)^2} + \left(\frac{\sigma_a}{a} \right)^2 \right]^{1/2} \quad (B2)$$

The errors associated with the standard deviations are 2.5% in thermal conductivity, 0.1 C in all temperatures out of an average of 20 C temperature difference, and 0.2% in wall thickness. The net result is an estimated relative RMS error of $\pm 3\%$ in the heat transfer coefficient.

APPENDIX A. Modified Boussinesq Approximation.

It is traditional that nondimensionalization of the momentum equation for the case of free convection on vertical or inclined boundaries results in the Grashof number

$$Gr = \frac{g \rho (\rho_\infty - \rho) x^3}{\mu^2} \quad (A1)$$

representing a dimensionless difference in pressure gradient in the direction perpendicular to effective gravitational forces. The usual Boussinesq approximation applies to single phase boundary layers and puts the density difference in terms of the thermal expansion coefficient such that

$$\rho - \rho_\infty = \rho \beta (T_\infty - T) \quad (A2)$$

In the case of two-phase fluid, the transverse difference in pressure gradients is due to the difference between the film density and that of the bulk fluid given by

$$\rho - \rho_\infty = \rho - [(1-\alpha)\rho_L + \alpha\rho_V] \quad (A3)$$

If the liquid density difference is now expressed through (A2) and (A3) rearranged, the result is

$$\rho - \rho_\infty = \rho \beta (T_\infty - T_L) + \alpha (\rho_L - \rho_V) \quad (A4)$$

Except for extremely low void fractions of the order of 2% or less, the thermal expansion effects are far outweighed by the voiding effects and were neglected. Similarly, for most systems of interest $\rho_f \gg \rho_g$ so that (A1) then becomes

$$Gr = \frac{g \alpha x^3}{\nu^2} \quad (A5)$$

APPENDIX B. Error Estimate for Heat Transfer Coefficient.

For any variable ψ , the relative expected standard deviation is given by

$$\frac{\sigma_\psi}{\psi} = \sqrt{\sum_i \frac{1}{\psi} \left(\frac{\partial \psi}{\partial X_i} \sigma_{X_i} \right)^2} \quad (B1)$$

where X_i are the independent parameters associated with the computation of ψ . From Equation (4) we easily find that

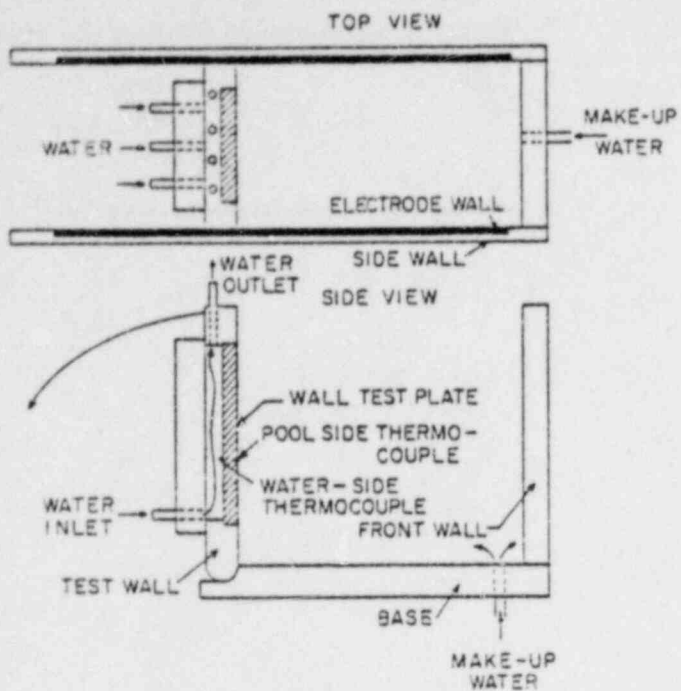


Figure 1. Schematic of Test Apparatus.

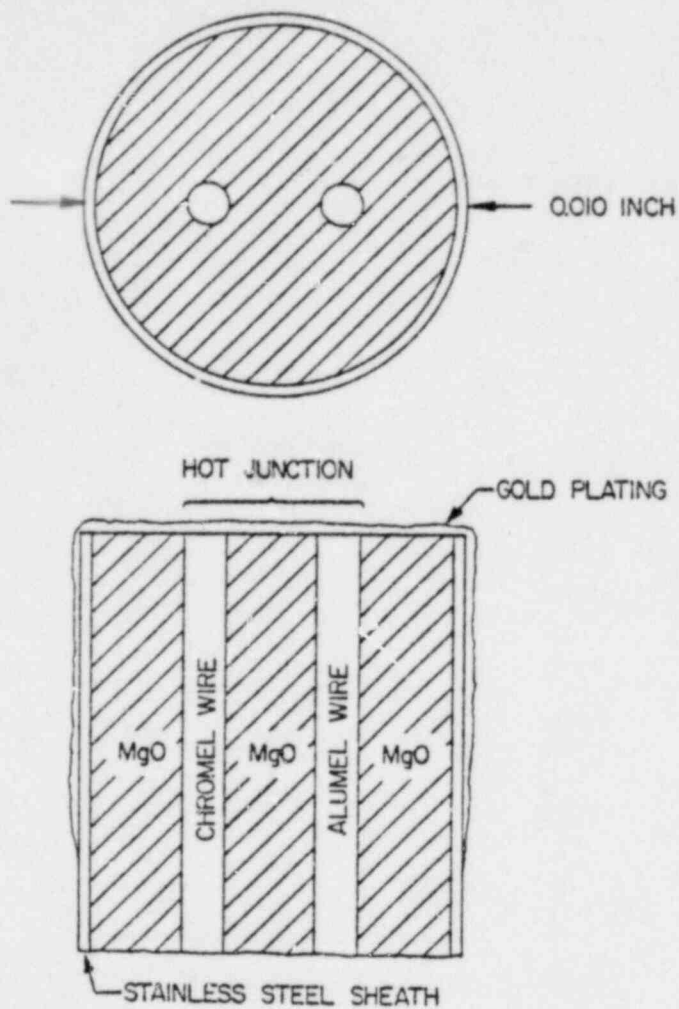


Figure 2. Schematic View of Gold-Plated Microthermocouple.

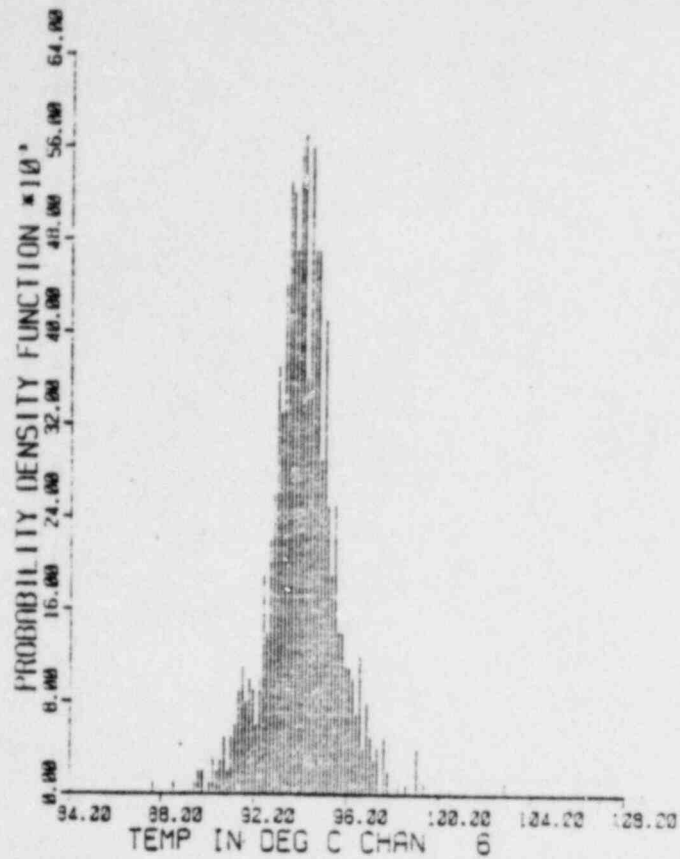


Figure 3. Histogram of Pool-Side Wall Temperature Fluctuations in the Bubbly Flow Regime.

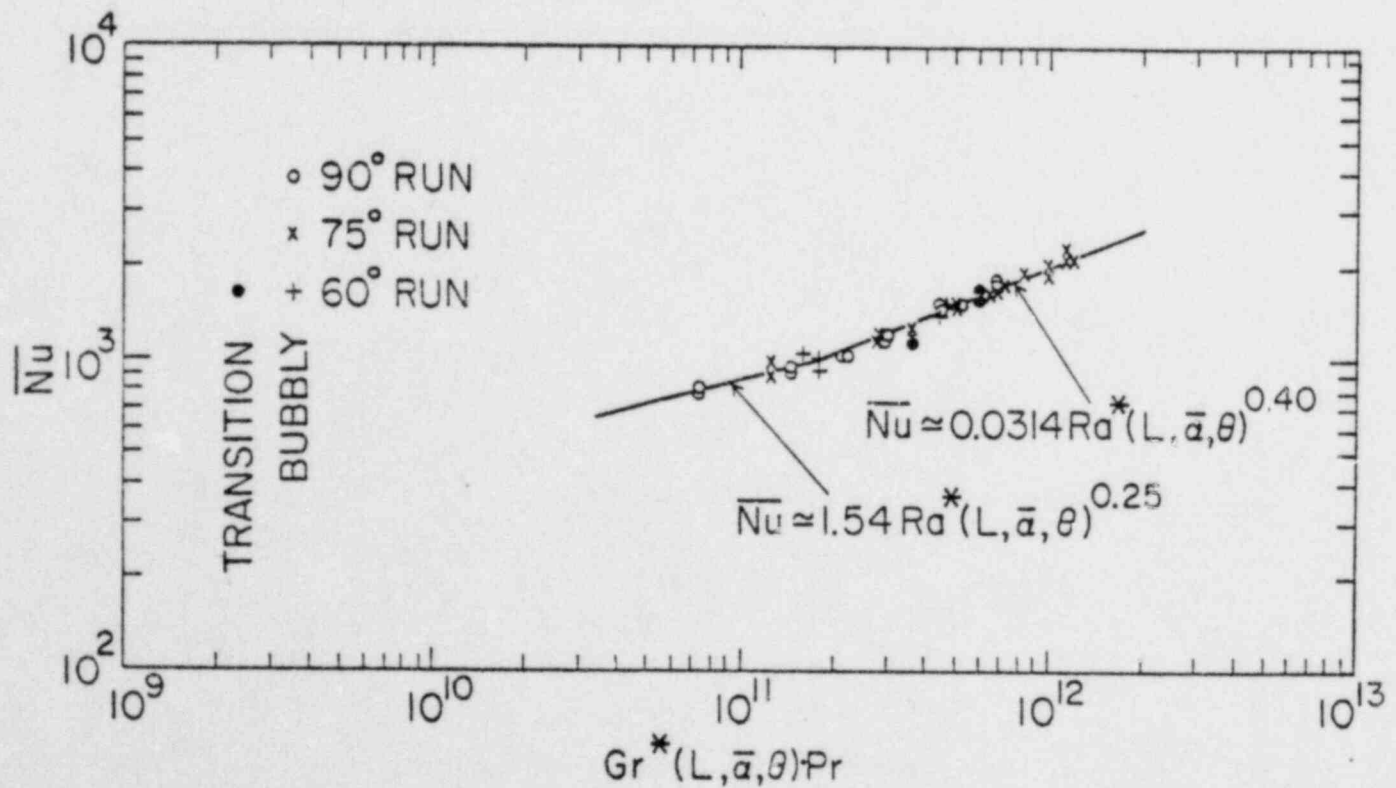


Figure 4. Modified Natural Convection Correlation of Average Heat Transfer Data for Three Wall Angles in the Bubbly Flow Regime.

TABLE 1
SUMMARY OF LOCAL AND AVERAGE MODIFIED NATURAL CONVECTION CORRELATIONS.

Investigator	Local or Average	Wall Angle	Best Fit Correlation	Standard Deviation	Range of Applicability
Gustavson (3)	Local	Vertical	$Nu(x) = .78 Ra^{0.25}$	$\pm .35$	$Ra^* \leq 10^{12}$
	Average	Vertical	$\overline{Nu} = 1.07 Ra^{0.25}$	$\pm .30$	$Ra^* < 10^{12}$
Gabor (2)	Average	Vertical	$\overline{Nu} = 1.59 Ra^{0.25}$	$\pm .33$	$Ra^* < 2 \times 10^{12}$
		Vertical	or $\overline{Nu} = 1.42 Ra^{0.25}$	$\pm .25$	$Ra^* \leq 10^{11}$
			$\overline{Nu} = .0309 Ra^{0.40}$	$\pm .0058$	$Ra^* > 10^{11}$
Present Work	Local	90°	$Nu(x) = 1.40 Ra^{0.25}$	$\pm .23$	$Ra^* \leq 7 \times 10^{11}$
		75°	$Nu(x) = 1.47 Ra^{0.25}$		
		60°	$Nu(x) = 1.36 Ra^{0.25}$		
	Average	$90^\circ, 75^\circ, 60^\circ$	$Nu(x) = .0234 Ra^{0.40}$	$\pm .0020$	$Ra^* > 7 \times 10^{11}$
		$90^\circ, 75^\circ, 60^\circ$	$\overline{Nu} = 1.54 Ra^{0.25}$	$\pm .08$	$Ra^* \leq 1.9 \times 10^{11}$
		$90^\circ, 75^\circ, 60^\circ$	$\overline{Nu} = .0314 Ra^{0.40}$	$\pm .0016$	$Ra^* > 1.9 \times 10^{11}$